A Study on the Method to Reduce Thoracic Injury in Frontal Crash using Elderly Human and THOR FE Models

Kazunori Maehara
Yasuhiro Dokko
Honda R&D Co., Ltd.
Japan

Kazuki Ohhashi
Honda Techno Fort Co., Ltd.
Japan

Paper Number 23-0228

ABSTRACT

In Japan, the ratio of the elderly in traffic accident fatalities has been increasing, and the thorax is the most frequently injured body region. Therefore, preventing chest injury to the elderly is one of the key issues to achieve zero fatalities. For this reason, several detailed analyses of the chest injury mechanism have been performed using elderly human body models (HBM). In a previous study, under frontal crash condition, it was observed that the forward motion of the internal organ and the forward rotation of the upper torso push up the lower ribs, potentially leading to rib fractures. In this study, a novel occupant restraint concept was devised that could reduce chest injury due to the mechanism above, and its effectiveness was verified using an elderly HBM and THOR.

On the devised restraint system, a pair of shoulder belts that pass from left and right sides of the occupant shoulder to the same sides of flank were placed. The aim of them was dispersing the restraint force applied to the thorax of an occupant. A membrane was placed wrapping the abdomen between the two shoulder belts, which aimed to reduce the protrusion of the internal organ during a frontal crash.
For the devised restraint system, a series of CAE calculation using the elderly HBM was performed in the two crash conditions of FR56K and OMDB in comparison with the conventional 3P belt, and the effect for reducing the number of fractured ribs (NFR) was confirmed. Then, another series of CAE calculation using the THOR FE model was performed in the same conditions, and several chest injury criteria such as Rmax, PC Score, TIC_NFR, and TIC_NSFR were calculated. Finally, injury probabilities for these criteria of THOR and NFR of the HBM were compared.

Comparing the devised restraint system with the 3P belt, NFRs of the elderly HBM were significantly reduced, and all chest injury criteria of THOR were reduced, under both load cases.
In the OMDB condition using the devised system and THOR, The chest deflection at inner lower was the largest, and Rmax was relatively high than other chest injury criteria. In the same condition, TIC_NSFR showed the best correlation with the NFR of the elderly HBM.

It was considered the reason why Rmax was high on OMDB was that THOR had a more protruded ribcage around the lower region than the elderly HBM, which caused higher concentrated load on this region pushed by the shoulder belt.
The reason why the TIC_NSFR on OMDB was low was considered to be that the devised system restrained the chest evenly on the left and right, and the value of the term that indicates the left-right difference of the upper chest deflection in the TIC_NSFR formula became smaller.

It was found that the devised chest restraint system could significantly reduce rib fractures of the elderly HBM in a frontal crash.
It was also found that when the devised system was evaluated with THOR, every chest injury criterion was reduced.

INTRODUCTION

In recent years, population ratio of the elderly has been increasing in such developed countries as Japan. Therefore, a lot of elderly people get involved in traffic accidents. In Japan, the number of traffic accidents has been decreasing. But the ratio of the elderly (aged 65 years old and older) in traffic accident fatalities has been increasing [1]. The thoracic injury due to rib fracture is the main factor of the death of elderly people [2] [3]. One of the reasons for this is because the density and strength of bone decrease with age [4]. Therefore, preventing chest injury to elderly people is one of the key issues to achieve zero fatalities. For this reason, a lot of detailed analyses of the chest injury mechanism have been performed, using post-mortem human surrogates (PMHS) [5] [6] [7] [8] [9] and human body models (HBM) [10] [11] [12]. In the previous study by the authors, under frontal crash condition, it was observed that the forward motion of the internal organ and the forward rotation of the upper torso pushed up the lower ribs, potentially leading to rib fractures [13].
Under frontal crash condition, the current mainstream of the chest restraint method is the so-called three-point seatbelt (3P-belt), which uses a shoulder belt placed diagonally from one shoulder to the opposite side. Shaw et al. [14] mentioned that complex deformities of the thorax affect thoracic fractures and that asymmetric thoracic restraint morphology may be a factor of the complex deformity of the thorax, based on the results of the sled tests using PMHS. In the research for safer occupant restraint methods, several studies have been conducted in the past on chest restraint methods with different types of restraint system than the 3P-belt [15] [16] [17] [18] [19] [20] [21]. For example, Östling et al. [18] analyzed the use of a 3+2 Criss Cross belt, which is a normal 3P-belt with an additional shoulder belt in the opposite diagonal direction, and reported a reduction in the risk of chest injury.
On the other hand, Test device for Human Occupant Restraint (THOR) dummy has been developed to improve the biofidelity in various body regions including the chest [22] [23], and is implemented in some crash assessments. THOR is capable of measuring the 3D thorax deflection at four locations with a kind of light reflective displacement meter called the Infrared Telescoping Rod for Assessing of Chest Compression (IR-TRACC). Several chest injury criteria for the THOR dummy have been proposed (e.g.: Rmax, PC Score, TIC_NFR), using those four deflection measurements [24] [25] [26]. However, THOR and human body have more than four ribs. Kawabuchi et al. [12] showed by the analysis using the elderly HBM that correlation between the chest injury criterion which uses deflections of all ribs and the prediction of the number of fractured ribs is improved.
The THOR dummy has been used in some studies mentioned above on the chest restraint methods, but there is no comparison of several chest injury criteria for the THOR dummy in a chest restraint configuration that could reduce the chest injury. In this study, a novel occupant restraint concept was devised that could reduce the chest injury based on the mechanism of rib fractures, and its effectiveness was verified by comparing the number of rib fractures of the elderly HBM and several chest injury criteria for the THOR dummy under frontal crash conditions.

METHODS

Occupant FE Models

In this study an elderly occupant full body FE model (Figure 1 (a)) was used which is capable of predicting rib fracture has been developed by Ito et al.[27] [4] and Dokko et al.[28] [29]. The model was designed from the results of the average anthropometric measurement of American Male 50th percentile elderly human subjects. The age of the elderly occupant FE model is defined as 75 years old. Rib fracture was represented by the elimination of the elements reaching the fracture strain. The viscera were simplified and simulated in three groups of solid elements: thoracic viscera (mainly consisting of the lung and the heart), upper abdominal viscera (mainly consisting of the liver and the stomach), and lower abdominal viscera (mainly simulating the intestines). The upper and lower abdominal viscera were defined as incompressible materials, and their density distribution was set to reproduce the center of gravity of the actual human trunk. The THOR-50th Metric Version 1.4.1 (Figure 1 (b)) developed by Humanetics Inc. was used for the THOR FE model [30]. In this study the measurement points of chest deflection at upper-left, upper-right, lower-left and lower right were respectively named as UL, UR, LL and LR. LS-DYNA (Version971 R6.1.2) was adopted as a FEM solver [31].

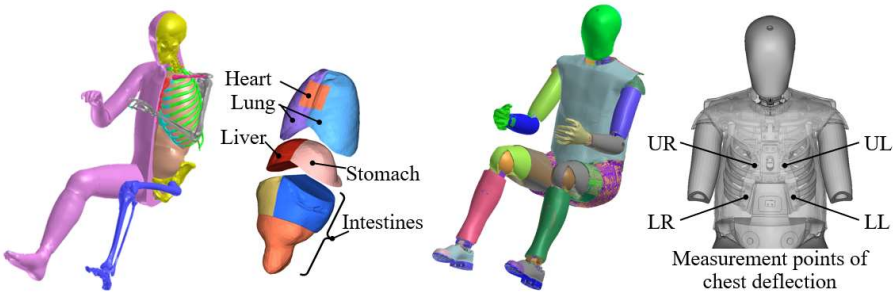

(a) Elderly occupant full body FE model (b) THOR-50th Metric Version 1.4.1

Figure 1. AM50 occupant FE model

As shown in Figure 2, in a full vehicle FE model, the elderly HBM and the THOR model were seated in the driver seat of a left-hand midsize sedan vehicle. As the baseline model, the vehicle model was equipped with a 3P-belt that had a force limiter, an anchor pretensioner, a retractor pretensioner, a knee airbag, and a side curtain airbag. The six-axis vehicle crash motions from the full frontal rigid barrier (FR56K) and the oblique moving deformable barrier (OMDB) tests [32] were applied. The body deformation of the vehicle was not simulated.

(a) Elderly HBM (b) THOR model

Figure 2. Occupant and Full vehicle FE model

The elderly HBM and the THOR model were both seated according to THOR seating procedure [32]. Figure 3 shows the postures of the elderly HBM and the THOR model.

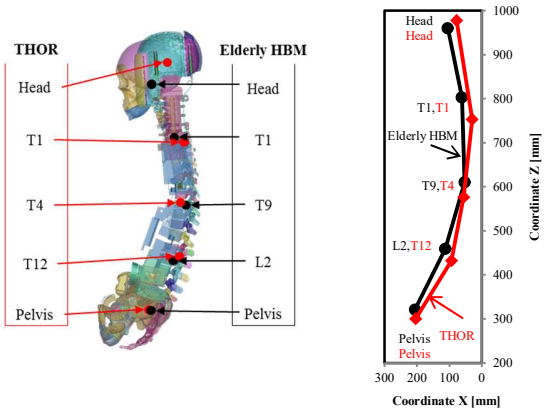

Figure 3. Posture of the elderly HBM and THOR models

Devised restraint system

Figure 4 shows the devised restraint system to reduce the chest injury. A pair of parallel shoulder belts, a membrane around the abdomen, and a 2P lap belt with an anchor pretensioner were equipped. The shoulder

belts aim to disperse the restraint force applied to the occupant thorax, by restraining both sides of the occupant shoulder. Four ends of both shoulder belts were attached to the retractors with pretensioners and force limiters, and these retractors were attached to the frame of the seat back. These parts of this restraint system were named as Twin Array Shoulder restraint KIt (TASKI), which in Japanese stands for a "cord used to tuck up the sleeves of a kimono". The aim of the membrane is reducing the protrusion of the internal organ during a frontal crash, named as Harness ARound Abdomen to Minimize Abdominal Kinetic Impact (HARAMAKI), which in Japanese stands for a "belly band". The whole restraint system illustrated in Figure 4 was named as TASKI+HARAMAKI. To make comparison with the baseline model, TASKI+HARAMAKI was implemented by replacing with the 3P-belt system, on both the elderly HBM and the THOR model, and in both FR56K and OMDB conditions.

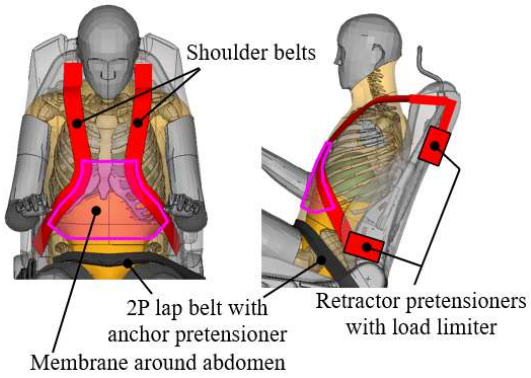

Figure 4. Schematic of the devised restraint system

Chest injury criteria for THOR dummy

In this study, Rmax, PC Score, TIC_NFR and TIC_NSFR were calculated from the results of the THOR model. Equations 1 to 4 respectively show the formulas of these chest injury criteria. Rmax is the maximum resultant deflection of the four measurements. PC Score was developed from a principal componet analysis (PCA) of a series of paird sled tests using PMHS and the THOR dummy. The formula of TIC_NFR and TIC_NSFR are consisted with a linear combination of the maximum of the four chest resultant deflections and the absolute value of the difference of the upper right and left deflections. TIC_NFR is the criterion of the number of all fractured ribs, and TIC_NSFR is that of the number of separated fractured ribs. Figure 5 shows the risk curves of AIS3+ and 65yo for these criteria. The risk curve for Rmax developed by Poplin et. al. [25] was chosen for this study.

$$R_{max} = \max\left(UL_{max}, UR_{max}, LL_{max}, LR_{max}\right)$$

$$\text{where } \left[\frac{U}{L}\middle|\frac{R}{L}\right]_{max} = \max\left(\sqrt{\left[\frac{L}{R}\right]X^2_{\left[\frac{U}{L}\right]S} + \left[\frac{L}{R}\right]Y^2_{\left[\frac{U}{L}\right]S} + \left[\frac{L}{R}\right]Z^2_{\left[\frac{U}{L}\right]S}}\right) \quad \text{Equation (1)}$$

$$PC\ Score = 0.486\left(\frac{up_{tot}}{17.439}\right) + 0.492\left(\frac{low_{tot}}{14.735}\right) + 0.496\left(\frac{up_{dif}}{9.672}\right) + 0.526\left(\frac{low_{dif}}{12.384}\right)$$

where

$up_{tot} = |UL|_{max} + |UR|_{max}$

$up_{dif} = |UL - UR|_{max}$

$low_{tot} = |LL|_{max} + |LR|_{max}$

$low_{dif} = |LL - LR|_{max}$ Equation (2)

$$TIC\_NFR = R_{max} + 1.66\ up_{dif} \quad \text{Equation (3)}$$

$$TIC\_NSFR = R_{max} + 3\ up_{dif} \quad \text{Equation (4)}$$

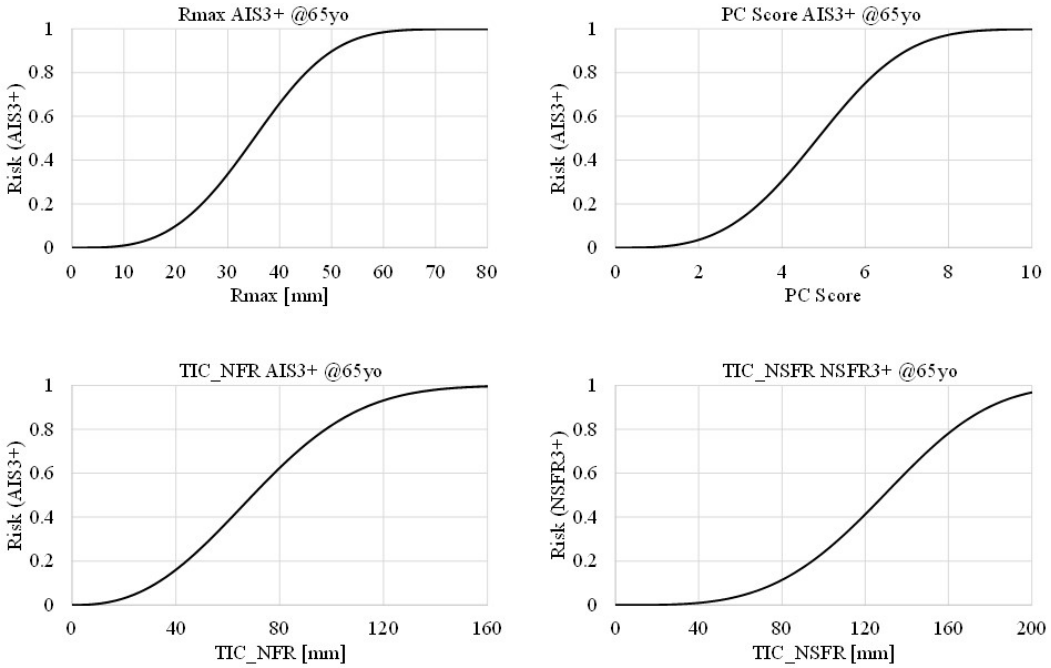

Figure 5. The risk curves of AIS3+ and 65yo of Rmax, PC Score, TIC_NFR and TIC_NSFR

Other candidates as chest injury predictor

In this study, additional two types of physical quantities were calculated as candidates of chest injury predictor. Both of them used physical quantities of all ribs, because it is considered that if fracture to each of all ribs can be taken into consideration, the number of fractures seems to be predicted more accurately.

One of them is a set of maximum rib strains of all ribs. In the case of a single rib on one side, a rib strain exceeding a certain value for the THOR dummy is considered to indicate the occurrence of a rib fracture in the human body. This concept was proposed by Davidsson et al. [33] [34]. Figure 6 shows the locations where the rib strains were measured. If a single rib of the THOR dummy is considered as a curved beam, the point of maximum bending moment is most likely to occur at the center of the curved beam. Therefore, the tensile strain along the longitudal direction at the outermost left and right sides of each rib were calculated from the THOR dummy model.

Another one is a set of normalized rib deflections of all ribs. Equation 5 shows the formula of the normalized rib deflection. The deflection of the THOR dummy is divided by the initial length of the rib, because the magnitude of the rib deflection of the THOR dummy contributing to the rib fractures in the human body is considered to depend on each size of the THOR ribs.

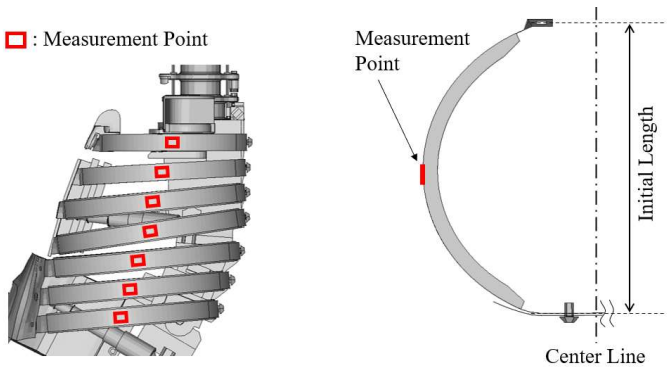

(a) Left View (b) Planner View of Rib #3

Figure 6. Measurement locations of rib strains on THOR dummy

$$\text{normalized rib deflection} = \frac{d_i}{L_i} \qquad \text{Equation (5)}$$

where di = deflection of each rib
Li = rib initial length

Procedure for evaluating the effectiveness of chest injury reduction

Table 1 shows the matrix of model conditions calculated in this study. Calculations were first performed using the elderly HBM with the 3P-belt and the devised restraint system under FR56k and OMDB conditions. From these results, the fracture locations and the number of fractured ribs were obtained. Secondly, calculations were conducted by replacing the elderly HBM with the THOR dummy model. From these results, Rmax, PC Score, TIC_NFR and TIC_NSFR were calculated, and obtained risks of AIS3+ at 65yo were compared with the number of fractured ribs of the elderly HBM. Then, the set of maximum rib strains of all ribs and that of normalized rib deflections of all ribs were graphed and compared with the fracture locations of the elderly HBM.

Table 1. Matrix of model conditions calculated in this study

Model #	Occupant Model	Crash Condition	Restraint System
1	elderly HBM	FR56K	3P-belt
2	elderly HBM	OMDB	3P-belt
3	elderly HBM	FR56K	devised restraint system
4	elderly HBM	OMDB	devised restraint system
5	THOR model	FR56K	3P-belt
6	THOR model	OMDB	3P-belt
7	THOR model	FR56K	devised restraint system
8	THOR model	OMDB	devised restraint system

RESULTS

Rib fracture locations and number of fractured ribs on elderly HBM

Figure 7 illustrates the locations of rib fracture of the elderly HBM in FR56K and OMDB conditions. Table 2 shows the number of fractured ribs in each model. With the 3P-belt, rib fractures were located around the path of the shoulder belt in FR56K. In OMDB, the number of fractured ribs increased to 16. It was observed that the upper torso of the elderly HBM contacted with the door lining as shown in Figure 8(a). With the devised restraint system, no rib fracture was observed either FR56K or OMDB condition. In OMDB condition, occupant's contact with the door lining was mitigated as shown in Figure 8(b). Figure 9 shows the deformed shapes of rib cage and viscera in FR56K condition, with fixed view on T10 vertebra. With the 3P-belt, forward movement of the internal organ was observed, which resulted in complex deformation of the ribcage. With the devised restraint system, forward movement of the internal organ was smaller than that of the 3P-belt, which resulted in less deformation of the ribcage, in combination with the effect of the dispersion of the restraint force on the chest.

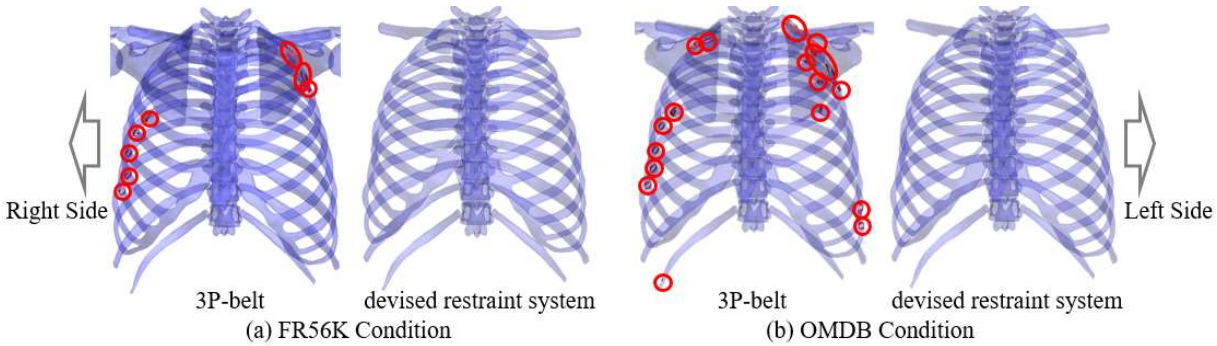

Figure 7. The locations of rib fracture of the elderly HBM in FR56K and OMDB conditions

Table 2. The number of fractured ribs of the elderly HBM in FR56K and OMDB conditions

	Number of Fractured Rib		
Model #	Left	Right	Total
1 (FR56K 3P-belt)	3	5	8
2 (OMDB 3P-belt)	8	8	16
3 (FR56K devised restraint system)	0	0	0
4 (OMDB devised restraint system)	0	0	0

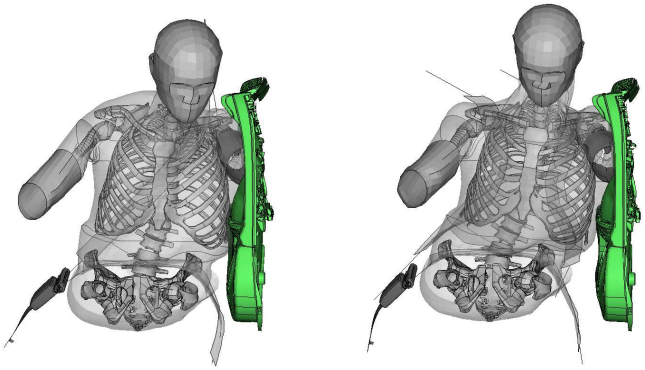

(a) 3P-Belt (b) The devised restraint system

Figure 8. The deformed body shapes and the door lining from the viewpoint of the vehicle coordinate system in OMDB condition

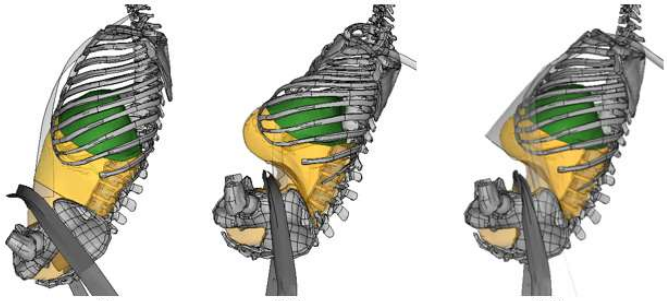

Figure 9. Left side view of deformation of rib cage and viscera (fixed view on T10 vertebra)

Chest injury criteria and risks of AIS3+ at 65yo on THOR dummy

Table 3 shows the maximum chest deflections of the four measurements on the THOR model. With the 3P-belt, the location of the highest chest deflection was obtained at UR in either FR56K or OMDB condition. With the devised restraint system, the value of the chest deflection at UR decreased in either FR56K or OMDB condition. But the deflection at LR in OMDB condition increased and became the highest of the four locations, in contrast with the result of the number of fractured ribs using the elderly HBM. Table 4 shows the chest injury criteria and the risks of AIS3+ at 65yo calculated from the results of the THOR model. For all chest injury criteria, the risks decreased between 3P-belt and the devised restraint system. But, in OMDB condition, the risks of Rmax and PC Score with the devised restraint system were greater than 50%, despite that the number of fractured ribs with the elderly HBM significantly decreased. The risks of TIC_NFR and TIC_NSFR with the devised restraint system were relatively low compared with those of Rmax and PC Score.

Table 3. The maximum chest deflections of four measurement on THOR model

Model #	UL	UR	LL	LR
5 (FR56K 3P-belt)	17.0	40.4	12.7	30.2
6 (OMDB 3P-belt)	28.8	52.2	22.8	36.4
7 (FR56K devised restraint system)	23.2	23.8	16.4	18.3
8 (OMDB devised restraint system)	25.6	33.6	30.4	42.5

Table 4. The chest injury criteria and the risks of AIS3+ at 65yo calculated from the results of THOR model

	Rmax		PC Score		TIC NFR		TIC NSFR	
Model #	Value	P(AIS3+)	Value	P(AIS3+)	Value	P(AIS3+)	Value	P(NSFR3+)
5 (FR56K 3P-belt)	40.4	67.3%	5.37	61.9%	80.8	63.4%	113.4	35.2%
6 (OMDB 3P-belt)	52.2	92.8%	7.15	91.8%	100.7	82.4%	139.9	60.7%
7 (FR56K devised restraint system)	23.8	17.2%	2.85	11.1%	29.9	8.1%	34.7	0.6%
8 (OMDB devised restraint system)	42.5	73.5%	5.10	55.8%	56.3	33.6%	67.4	6.3%

Results of other candidate as chest injury predictor

Figure 10 shows the graph of the maximum rib strains of all ribs. The vertical axis shows the rib number of the THOR dummy. The horisontal axis shows the maximum strain of each rib. For clarity, the horizontal axes on the right and left sides are reversed. In all conditions, the strain value of rib #1 of both side were higher than other ribs, and that of rib #3 and above had a tend to be higher than that of rib #4 and below.

With the 3P-belt, strain values on the right side are higher than that on the left side. Figure 11 shows the shoulder belt path of 3P-belt over the THOR dummy. The shoulder belt passes over the left rib #1 and right ribs from #2 to #7. So these ribs were pushed by the shoulder belt during crash, which resulted in relatively high strain values. The strain values of these ribs in OMDB condition are higher than that in FR55K condition.

With the devised restraint system, in both FR56K and OMDB condition, the strain values of the ribs where the shoulder belt passes over in the 3P-belt decreased, esecially with the right ribs from #4 to #7. The strain values of the left ribs from #3 to #7 increased, but remain around the same level as the opposite side.

Figure 12 shows the graph of normalized rib deflections of all ribs. These are graphed with the same manner as the maximum rib strains of all ribs. Overall, These graphs are simmiler to that of the maximum rib strains of all ribs. With the devised restraint system and in OMDB condition, however, the value of the normalized deflection of the right ribs from #5 to #7 increased, in contrast with the graph of the maximum rib strain of all ribs.

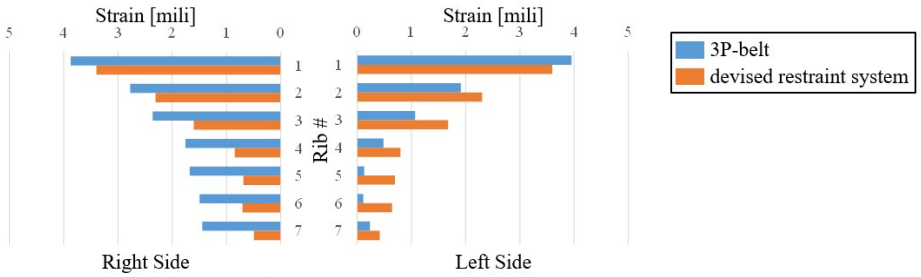

(a) FR56K

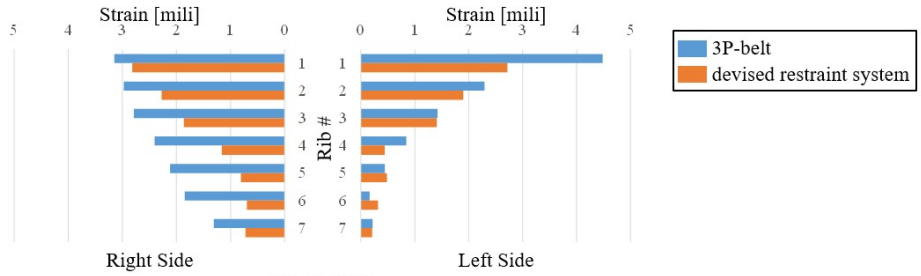

(B) OMDB

Figure 10. The graph of maximum rib strains of all ribs

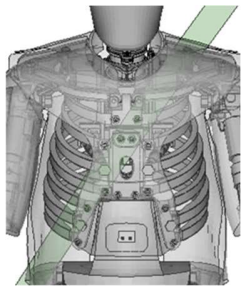

Figure 11. The shoulder belt path of 3P-belt over the THOR dummy

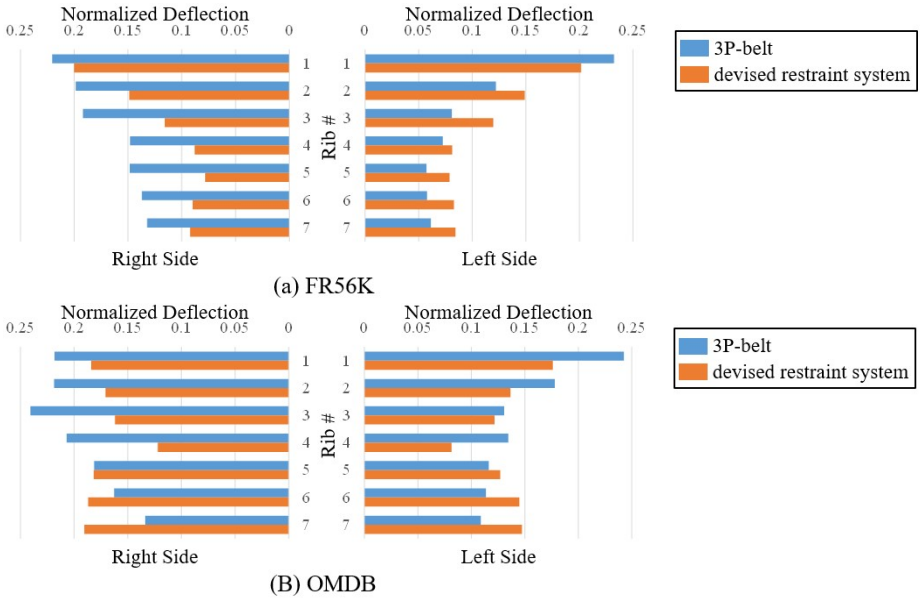

Figure 12. The graph of normalized rib deflections of all ribs

DISCUSSION

Chest deflection of lower rib on THOR dummy

With the devised restraint system, the deflection at LR in OMDB condition increased, in contrast with the result of the number of fractured ribs using the elderly HBM. Figure 13 shows the time histories of the resultant deflection and its components at LR in OMDB condition with the devised restraint system. The Z component has a positive peak which means downward. Figure 14 shows a comparison of the thorax shape of the elderly HBM and the THOR model, viewed from the right side. The lower part of the thorax of the THOR dummy protrudes forward compared to the elderly HBM. Therefore, it is thought that the protruding portion of THOR dummy is more easily pushed in by the belt than the elderly HBM. Figure 15 shows the right side view of the kinematics at 45ms and 90ms in OMDB condition with the devised restraint system. Between these times, the vehicle's floor moved downward, and the protruding portion of THOR dummy was pulled downward by the lower shoulder belts of the devised restraint system, which would cause the relatively large chest deflection with the THOR model. This tendency of the greater deflection of the lower ribs influences the results with higher risks for Rmax and PC Score in the OMDB condition. On the other hand, TIC_NFR and TIC_NSFR have lower risks. The reason for this may be that the equations of those are linear combinations of the Rmax and left-right differences in the upper deflection, and include a term that gives weight to the upper deflection value, which relatively reduces the influence of the lower rib value.

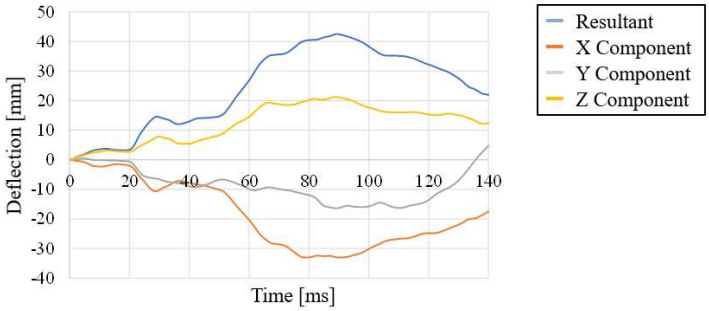

Figure 13. The time histories of the resultant deflection and its components at lower-right in OMDB condition with the devised restraint system.

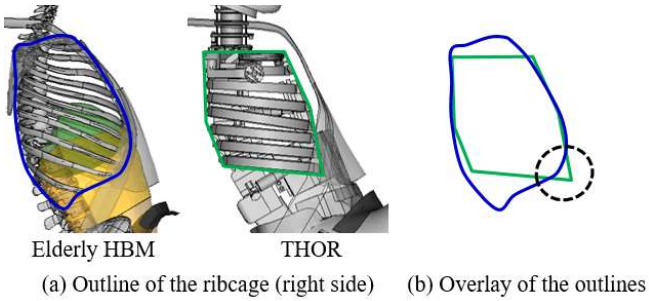

Figure 14. Illustration of a comparison of the thorax shapes of the elderly HBM and the THOR model (viewed from the right side)

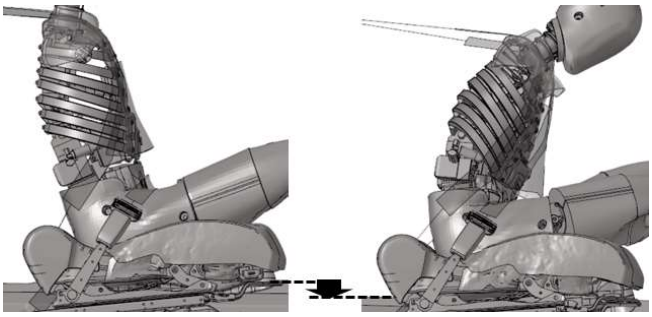

Figure 15. The right side view of the result animation in OMDB condition with the devised restraint system

Normalized cord deflections of all ribs

The graph of the maximum rib strain of all ribs seems to well represent the increase and decrease of the number of fractured ribs of the elderly HBM. On the other hand, the graph of the normalized rib deflections of all ribs has discrepancy with the number of fractured ribs of the elderly HBM with the devised restraint system and in OMDB condition. This is because of the tendency of greater deflection of the lower ribs of the THOR dummy mentioned above. Here, the structure of an actual human body around the connection between the rib and the thoracic vertebrae was considered. Figure 16 shows the schematic of costovertebral joint in a human body. This joint moves during respiration. The degree of freedom of this joint allow the anterior end of the ribs to move up and down to some extent. Therefore, the Z component of the chest deflection of the THOR dummy is expected to have little effect on the rib deformations and fractures in a human body. So, the deflection value used in that graph was exchanged from 3D deflection to cord deflection, for the purpose of reducing the influence of the Z component of the rib deflection. Figure 17 shows the illustration of the cord deflection of the THOR dummy. The cord length was measured by the distance between the anterior and posterior holes of the rib on one side. Then, the cord deflection was calculated as the change in the cord length. Figure 18 shows the graph of the normalized cord

deflections of all ribs. In this graph, the maximum cord deflection was divided by the initial value of the cord length. Overall, this graph is similar to the graph of the maximum rib strain of all ribs, and with the devised restraint system and in OMDB condition, the value of the right ribs from #5 to #7 decreased, which seems to well represent the result of the elderly HBM.

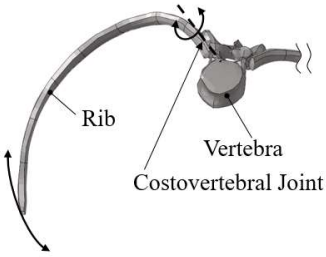

Figure 16. The schematic of costovertebral joint in the human body

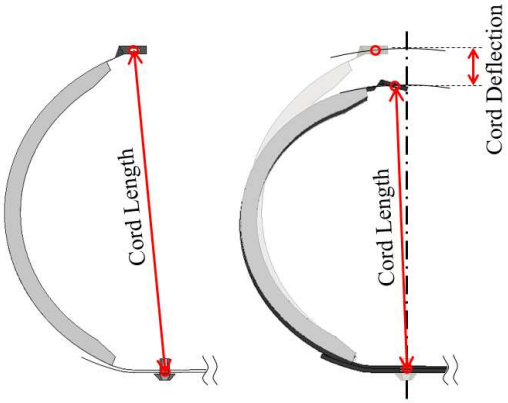

Figure 17. The illustration of the cord deflection of the THOR dummy

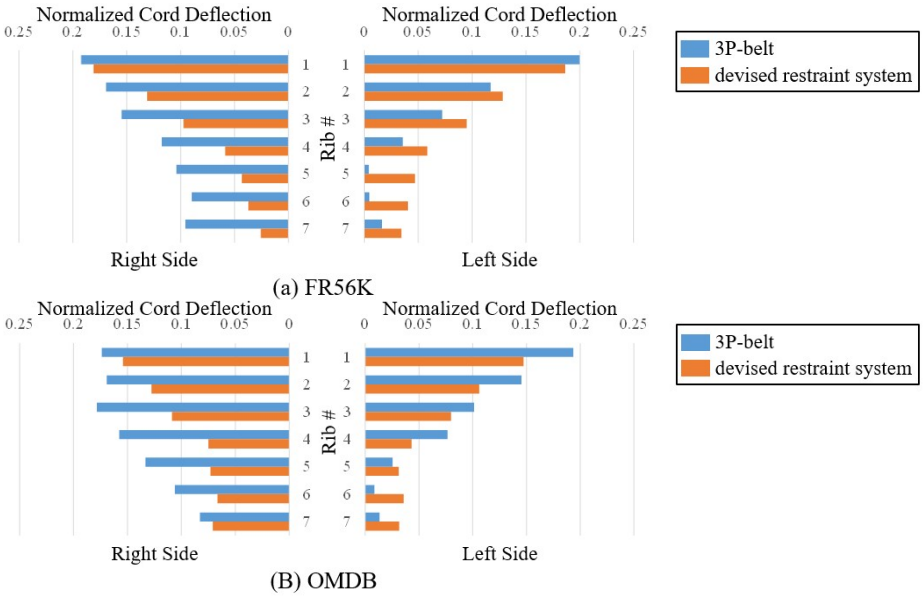

Figure 18. The graph of the normalized cord deflections of all ribs

CONCLUSION

In this study, a novel occupant restraint concept was devised that could reduce the chest injury based on the mechanism of rib fractures in FR56K and OMDB conditions, and its effectiveness was verified by comparing the number of rib fractures of the elderly HBM and several chest injury criteria for the THOR dummy. Additionally, some candidates as the chest injury predictor using all ribs of the THOR dummy were graphed and compared with the fracture locations of the elderly HBM.

As the results, the following conclusions were obtained.

・By implementing the devised restraint system, the number of fractured rib was significantly decreased in the elderly HBM.

・In the THOR model, the risks of rib fracture predicted by all of the chest injury criteria calculated in this study decreased with the devised restraint system. However, the extent of the reduction varied widely among the chest injury criteria, especially in OMDB condition.

REFERENCES

[1] Cabinet Office, “White Paper ON Traffic Safety in Japan 2021 2/3”, https://www8.cao.go.jp/koutu/taisaku/r03kou_haku/english/pdf/wp2021-2.pdf, 2022

[2] Kent, R. et al., “Fatality risk and the presence of rib fractures”, 52nd AAAM Annual Conference, p.73–84, 2008

[3] Cuerden R. et al., “An Estimation of the Costs and Benefits of Improved Car to Car Compatibility on a National and European Scale”, VC Compat Growth project GRD2-2001-50083, Deliverable D24, 2006

[4] Ito, O. et al., “Development of adult and elderly FE thorax skeletal models”, SAE Technical Paper 2009-01-0381, 2009

[5] Kemper, A. et al., “Material Properties of Human Rib Cortical Bone From Dynamic Tension Coupon Testing”, STAPP Car Crash Journal, vol.49, p.199-230, 2005

[6] Kemper, A. et al., “The Biomechanics of Human Ribs: Material and Structural Properties From Dynamic Tension and Bending Tests”, STAPP Car Crash Journal, vol.51, p.235-273, 2007

[7] Kindig, M. et al., “The influence of geometry on the biomechanical response of human ribs under frontal loading”, M.S. Thesis, University of Virginia, 2009

[8] Kent, R. et al., “Frontal Thoracic Response to Dynamic Loading: the Role of Superficial Tissues, Viscera, and the Rib Cage”, IRCOBI Annual Proceedings, 2005

[9] Lessley, D. J. et al., "Kinematics of the Thorax under Dynamic Belt Loading Conditions", International Journal of Crashworthiness, Vol.15, No.2, p.175-190, 2010

[10] Ito, Y. et al., “Response Analysis of Thoracic Rib-Cage against Blunt Loading Using Human Elderly FE Model”, Transactions of Society of Automotive Engineers of Japan, 2012

[11] Maehara, K. et al., “A Study on the Biofiderity of the Thorax Response of the Next-generation Frontal Crash Test Dummy THOR”, Transactions of Society of Automotive Engineers of Japan, 2018

[12] Kawabuchi, T. et al., “EVALUATION OF THORACIC DEFLECTION CRITERIA IN FRONTAL COLLISION USING THORACIC IMPACTOR SIMULATION WITH HUMAN BODY FE MODEL”, 26th ESV Conference, Paper No. 19-0068, 2019

[13] Maehara, K. et al., “On the Effect of the Interaction between the Thoracoabdominal Wall and the Viscera to Thoracic Injury in Frontal Crash”, Proceedings, 2020 JSAE Annual Congress (Spring), 2020

[14] Shaw, G. et al., “Impact Response of Restrained PMHS in Frontal Sled Tests: Skeletal Deformation Patterns Under Seat Belt Loading”, STAPP Car Crash Journal, Vol.53, p.1-48, 2009

[15] Rouhana, S. W. et al., “Biomechanics of 4-Point Seat Belt System in Frontal Impacts”, STAPP Car Crash Journal, Vol.47, p.367-399, 2003

[16] Bostrom, O. et al., “BENEFITS OF A 3+2 POINT BELT SYSTEM AND AN INBOARD TORSO SIDE SUPPORT IN FRONTAL, FAR-SIDE AND ROLLOVER CRASHES”, 18th ESV Conference, Paper No.451, 2003

[17] Bostrom, O. et al., “MECHANISM OF REDUCING THORACIC DEFLECTIONS AND RIB STRAINS USING SUPPLEMENTAL SHOULDER BELTS DURING FRONTAL IMPACTS”, 18th ESV Conference, Paper No.13-0372, 2013

[18] Östling, M. et al., “Potential Benefit of a 3+2 Criss Cross Seat Belt System in Frontal and Oblique Crashes”, IRCOBI Conference 2017, IRC-17-57, 2017

[19] Mroz, K. et al., “Evaluation of Adaptive Belt Restraint Systems for the Protection of Elderly Occupants in Frontal Impacts”, IRCOBI conference 2018, IRC-18-15, 2018

[20] Mizuno, K. et al., “Study of seatbelt system for reduction of chest deflection”, Proceedings, 2018 JSAE Annual Congress (Spring), 2018
[21] Hu, J. et al., “A New Prototype 4‐Point Seatbelt Design to Help Improve Occupant Protection in Frontal Oblique Crashes”, IRCOBI conference 2018, IRC-18-18, 2018
[22] Ridella, S. A. and Parent, D. P., “MODIFICATIONS TO IMPROVE THE DURABILITY, USABILITY AND BIOFIDELITY OF THE THOR-NT DUMMY”, 22nd ESV Conference, Paper Number 11-0313, 2011
[23] Lemmen, P. et al., “AN ADVANCED THORAX-SHOULDER DESIGN FOR THE THOR DUMMY”, 23rd ESV Conference, Paper Number 13-0171, 2013
[24] Crandall, J., “Injury Criteria Development: THOR Metric SD-3 Shoulder Advanced Frontal Crash Test Dummy,” NHTSA Biomechanics Database, Report b11117-1, 2013
[25] Poplin, G. S. et al., “Development of thoracic injury risk functions for the THOR ATD”, Accident Analysis and Prevention, Volume106, p.122-130, 2017
[26] Trosseille, X. et al., “Assessment of Several THOR Thoracic Injury Criteria based on a New Post Mortem Human Subject Test Series and Recommendations”, Stapp Car Crash Journal, Vol. 63, pp. 291-305, 2019
[27] Ito, O. et al., “Development of the Human Lower Limb FE Models of Adult and Elderly Person Considering Aging Effects”, Proceedings, JSAE Annual Congress (Spring), 2008
[28] Dokko, Y. et al., “Development of Human Lower Limb and Pelvis FE Models for Adult and the Elderly”, SAE Technical Paper 2009-01-0396, 2009
[29] Dokko, Y. et al., “Development of Human Lumbar Spine FE Models for Adult and the Elderly”, SAE Technical Paper 2009-01-0382, 2009
[30] HUMANETICS Innovative Solutions, “THOR-50th Metric V1.4.1 LS-DYNA Model Technical Report User’s Manual”, 2016
[31] LSTC, “LS-DYNA Version 971 R6 User’s Manual”, 2012
[32] U.S. Department of Transportation National Highway Traffic Safety Administration Office of Vehicle Safety Research, “ObliqueTestProcedureDraft”, 2015
[33] Davidsson, J. et al., “Set of injury risk curves for different sizes and ages”, Chalmers Publication Library, 2013
[34] Davidsson, J. et al., “Development of injury risk functions for use with the THORAX Demonstrator; an updated THOR”, IRCOBI Conference 2014, IRC-14-41, 2014